# Recovery of the Spatial State of the Ionosphere Using Regular Definitions of the TEC Identifier at the Network of Continuously Operating GNSS Stations of Ukraine

L. M. Yankiv-Vitkovska[1], S. H. Savchuk[1], V. K. Pauchok[2], Ya. M. Matviichuk[1], and D. I. Bodnar[2]

*1. Lviv Polytechnic National University*

*2. Ternopil National Economic University*

**Abstract:** We developed a system for monitoring the ionosphere, which uses the GNSS network located in the western part of Ukraine. The system is based on determining the ionosphere parameters from GNSS observations performed at an individual station. We are proposed algorithm for restoring the spatial position of the ionospheric state or its ionization field according to the regular definitions of the TEC parameter. The description below shows one of the possible solutions that are based on the application of the regularized approximation of functions with numerous variables. To experimentally determine the changes in the ionization field in time, we took measurements from 272 days in 2013 that were determined during the GNSS observations at 17 continuously operating stations of the ZAKPOS network. The resulting error indicators show that the developed algorithm gives consistent results for ionization field restoration that do not depend on the ionosphere state, satellites positions and changes in number of stations in the network used for computations.

**Key words:** Ionosphere, ionospheric parameters, GNSS-measurements, interpolation, regularized approximation, Spline approximation.

## 1. Introduction

Due to the wide application of global navigation satellite systems (GNSS), the development of the modern GNSS infrastructure moved the monitoring of the Earth's ionosphere to a new methodological and technological level. The peculiarity of such monitoring is that it allows conducting different experimental studies including the study of the ionosphere directly while using the existing networks of reference GNSS stations intended for solving other problems.

The application of the modern GNSS infrastructure is another innovative step in the ionospheric studies as such networks allow to conduct measurements continuously over time in any place. This is used during the monitoring of the ionosphere and allows

studying the global and regional phenomena in the ionosphere in real time.

Application of a network of continuously operating reference stations to determine numerical characteristics of the Earth's ionosphere allows creating an effective technology to monitor the ionosphere regionally. This technology is intended to solve both scientific problems concerning the space weather, and practical tasks such as providing coordinates of the geodetic level accuracy.

Thus, for the calculated numerical characteristics of the ionosphere that reflects the determined functional dependencies from the time [1, 2] of the individual system parameters and processes of different nature, a universal algorithm of regularized identification of mathematical macromodels was developed.

The practical implementation of this algorithm improves the processing of the measured data,

**Corresponding author:** Liubov Yankiv-Vitkovska, PhD, research fields: ionospere, GNNS-system.

monitoring tools, recovery of missed measured data and its prediction.

## 2. Formulation of the Problem

For continuously operating reference GNSS stations, the results of the determined ionization identifier *TEC* (Total Electron Content) that describes the number of ions in the atmosphere on the line between the ground station and the moving satellite accumulate. On the one hand, this data reflects the state of the ionosphere during the observation; on the other hand, it is a substantial tool for accuracy improvement and reliable determination of coordinates of the observation place.

Thus, it was decided to solve a problem of restoring the spatial position of the ionospheric state or its ionization field according to the regular definitions of the *TEC* identifier, i.e., *STEC* (Slant *TEC*). The description below shows one of the possible solutions that is based on the application of the regularized approximation of functions with numerous variables.

Initial data to restore the ionization field:

- coordinates of reference stations:

$$X_i^{st}(t_k), Y_i^{st}(t_k), Z_i^{st}(t_k) \; (i = \overline{1, n_k} \; ; \; k = \overline{1, K} \,), \text{(1a)}$$

- coordinates of GNSS satellites:

$$X_j^{sp}(t_k), Y_j^{sp}(t_k), Z_j^{sp}(t_k) \, (j = \overline{1, m_k} \; ; \; k = \overline{1, K}), \text{(1b)}$$

- *STEC* values between the station *i* and satellite *j*:

$$s_{ij}(t_k) \; (i = \overline{1, n_k} \; ; \; j = \overline{1, m_k} \; ; \; k = \overline{1, K} \,), \text{(1c)}$$

where: $t_k$ – time of the *STEC* measurement; $K$ – number of measurements; $i$ – station number; $j$ – satellite number; $n_k$, $m_k$, – number of stations and satellites during the measurement k, respectively. Further, we used data from 19 reference stations in the Western Ukraine.

The solution to this problem is to define the ionization field

$$v = v(x, y, z, t)$$

for the area where the stations are located ($x$, $y$, $z$) during the time $t \in [t_1, t_K]$.

## 3. Restrictions and Assumptions for Use of the GNSS Measurements to Restore the Ionization Field

The coordinates of an individual station (1a) and available satellite *j* (1b) define the line segment that connects the point on the Earth's surface with the satellite. This line segment comes through the Earth's ionosphere as well. One of the assumptions in this case is that the ionosphere layer has an effective thickness that is defined by the sub-ionospheric point *H*. According to this assumption, all ionized atoms are located on the surface of some sphere with the radius defined by the sub-ionospheric point.

Let's divide the part of the specified line segment into *N-1* equal segments, thus, getting *N* equally located nodes that lie on a beam from the station to the satellite below the sub-ionospheric point (Fig. 1):

$$\overline{x}_{ijl}^k = \overline{x}_{ijl}(t_k)_{,} \; \overline{y}_{ijl}^k = \overline{y}_{ijl}(t_k)_{,} \; \overline{z}_{ijl}^k = \overline{z}_{ijl}(t_k)_{,} \text{(2)}$$

where: $\overline{x}_{ijl}^k$, $\overline{y}_{ijl}^k$, $\overline{z}_{ijl}^k$ are spatial coordinates of a point *l* on a beam between station *i* and satellite *j* ($i = \overline{1, n_k}$ ; $j = \overline{1, m_k}$ ; $l = \overline{1, N}$ ; $k = \overline{1, K}$ ).

Supposing that the state of the ionosphere changes evenly along the beam between the station and the satellite, the ionization field indicator in each node can be described as:
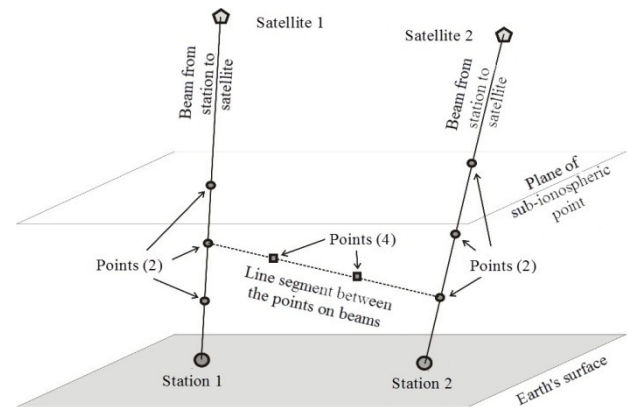


**Fig. 1   Spatial location of the nodes.**

$$\overline{v}_{ijl}^{k} = s_{ij}(t_k)/N \; (i=\overline{1,n_k}; \; j=\overline{1,m_k}; \; l=\overline{1,N}; \; k=\overline{1,K}), \; (3)$$

where $\overline{v}_{ijl}^{k}$ – ionization parameter in point $l$ on a beam between station $i$ and satellite $j$.

Expression 3 describes the ionization values determined experimentally. GNSS observations show that the beams from satellites to stations at one point in time lie mostly in certain directions only, while there are few of them that lie in other directions or none at all (Fig. 2).

This fact makes the conditions of the interpolation problem worse. For their improvement, we connected all the points (2) on the beams between the stations and satellites and on the formed line segments we defined internal equally located nodes that do not lie on the boundaries of the line segments (see Fig. 3):

$$\breve{x}_{ijpq}^{kr}, \; \breve{y}_{ijpq}^{kr}, \; \breve{z}_{ijpq}^{kr}, \qquad (4)$$

where: $\breve{x}_{ijpq}^{kr}$, $\breve{y}_{ijpq}^{kr}$, $\breve{z}_{ijpq}^{kr}$ — spatial coordinates of the point $r$ ($r = \overline{1,M}$) on the line segment between the nodes ($\overline{x}_{ijp}^{k}$, $\overline{y}_{ijp}^{k}$, $\overline{z}_{ijp}^{k}$), ($\overline{x}_{ijq}^{k}$, $\overline{y}_{ijq}^{k}$, $\overline{z}_{ijq}^{k}$); $p,q \in [1,N]$; $i=\overline{1,n_k}$; $j=\overline{1,m_k}$; $k=\overline{1,K}$; $M$ – number of internal nodes on a line segment between the points on the beam.
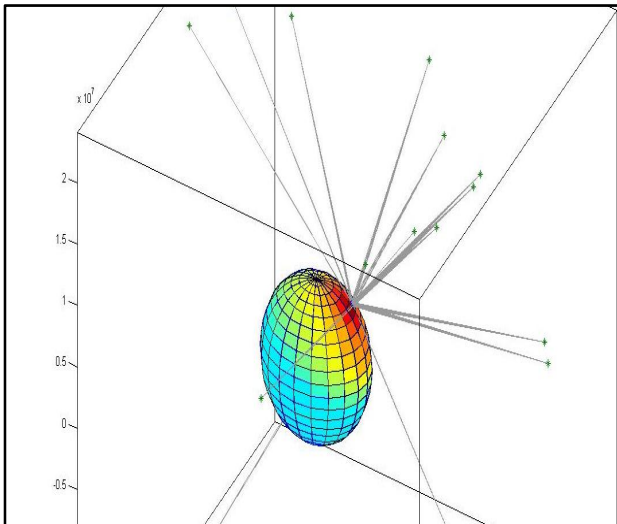


**Fig. 2 Common view of beams from the station to the satellites according to (1a) and (1b).**
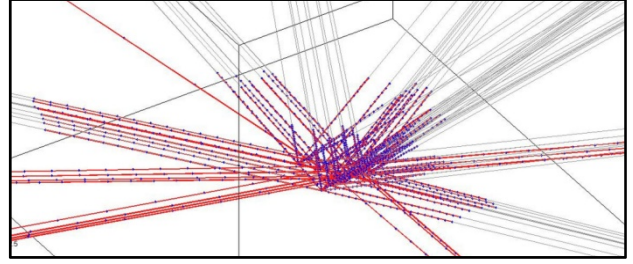


**Fig. 3 Beams from stations to satellites (in grey), their sub-ionospheric line segments (in red) and points (2) on them (in blue).**

Ionization parameters in the nodes (4) are defined using linear interpolation value of this indicator on a line segment between the points ($\overline{x}_{ijp}^{k}$, $\overline{y}_{ijp}^{k}$, $\overline{z}_{ijp}^{k}$), ($\overline{x}_{ijq}^{k}$, $\overline{y}_{ijq}^{k}$, $\overline{z}_{ijq}^{k}$); $p,q \in [1,N]$; $i=\overline{1,n_k}$; $j=\overline{1,m_k}$. It is described as:

$$\breve{v}_{ijpq}^{kr} \; (i=\overline{1,n_k}; \; j=\overline{1,m_k}; \; p,q \in [1,N]; r=\overline{1,M}; k=\overline{1,K}) \; (5)$$

Expression 3 describes ionization in the nodes (2) located along the beams between the stations and satellites. Expression 5 describes ionization in the nodes (4) that lie between such different beams. It was found that data from expressions 2-5 is not enough to restore the ionization field as approximating functions deviate greatly from the observational ionization values beyond the nodes (2), (5).

## 4. Description of the Method for Determining Ionization Using STEC

For practical purposes, we need to define ionization in the spatial area:

$$x \in [x_{min}^{k}, x_{max}^{k}], \; y \in [y_{min}^{k}, y_{max}^{k}], \; z \in [z_{min}^{k}, z_{max}^{k}] \; (6)$$

where the area boundaries are defined by the extreme points of the set of nodes (2) that are located on the beams between the stations and satellites:

$$x_{min}^{k} = \min_{ijl} \overline{x}_{ijl}^{k}; \; y_{min}^{k} = \min_{ijl} \overline{y}_{ijl}^{k}; \; z_{min}^{k} = \min_{ijl} \overline{z}_{ijl}^{k};$$

$$x_{max}^{k} = \max_{ijl} \overline{x}_{ijl}^{k}; \; y_{max}^{k} = \max_{ijl} \overline{y}_{ijl}^{k}; \; z_{max}^{k} = \max_{ijl} \overline{z}_{ijl}^{k}.$$

Let's divide line segments that describe the rectangular area (6) into *L-1*smaller segments and determine the coordinates of the equally located nodes:

$$\widehat{x}_i^k, \widehat{y}_j^k, \widehat{z}_l^k \ (i,j,l=\overline{1,L}). \quad (7)$$

To restore the ionization field in the area (6) according to the data from the expressions 2-5, a new condition needs to be imposed: ionization derivatives with respect to the coordinates must be minimal in the points (7). Such condition reduces strong deviations of the approximating function beyond the nodes (2), (4). It should be noted that the solution to the problem of the ionization field restoration lies in finding the ionization values in the nodes (7).

Set of the points (2), (4) coordinates is denoted by:

$$x_a^k=\left\{\overline{x}_{ijl}^k,\breve{x}_{ijpq}^{kr}\right\}, y_a^k=\left\{\overline{y}_{ijl}^k,\breve{y}_{ijpq}^{kr}\right\}, z_a^k=\left\{\overline{z}_{ijl}^k,\breve{z}_{ijpq}^{kr}\right\}, (8)$$

where: $a=\overline{1,A_k}$ ; $A$ – number of points in the expressions (2), (4) ($i=\overline{1,n_k}$ ; $j=\overline{1,m_k}$ ; $p,q\in[1,N]$ ; $r=\overline{1,M}$ ; $k=\overline{1,K}$ ).

Set of the ionization identifier values (3), (5) is denoted by:

$$v_a^k=\left\{\overline{v}_{ijl}^k,\breve{v}_{ijpq}^{kr}\right\}, \quad (9)$$

where: $a=\overline{1,A_k}$ ; $i=\overline{1,n_k}$ ; $j=\overline{1,m_k}$ ; $p,q\in[1,N]$ ; $r=\overline{1,M}$ ; $k=\overline{1,K}$ .

Sets (8), (9) define the discrete dependency of the ionization $v_a^k$ from the values of three spatial coordinates ( $x_a^k$ , $y_a^k$ , $z_a^k$ ) ( $a=\overline{1,A_k}$ ). This dependency is approximated by the exponential polynomial from numerous arguments:

$$v(x,y,x)=P_k(x,y,x).$$

During the calculations, such polynomials were selected:

$$P_k(x,y,x)=\sum\nolimits_{i+j+l<R}c_{ijl}^k x^i y^j z^l ;$$

$$P_k(x,y,x)=\sum\nolimits_{|i+j+l|<R}c_{ijl}^k x^i y^j z^l ;$$

$$P_k(x,y,z)=\sum\nolimits_{i+j+l<r}c_{ijl}^k x^{\lambda i} y^{\lambda j} z^{\lambda l} ;$$

$$P_k(x,y,z)=\sum\nolimits_{|i+j+l|<R}c_{ijl}^k x^{\lambda i} y^{\lambda j} z^{\lambda l} ,$$

where: $R$ – exponent of polynomial ($R=1,\ldots,4$)); $c_I^k$ – coefficients of this polynomial, $I$ – multi-indexes of these coefficients; $\lambda$ – number close to $R$ ($\lambda\in[R-0.3;R+0.3]$). Polynomial with random exponents was also selected:

$$P_k(x,y,z)=\sum c_{\xi_x\xi_y\xi_z}^k x^{\xi_x} y^{\xi_z} z^{\xi_z} ,$$

where $\xi_i$ (i = x, y, z) equally distributed random numbers. In particular, exponents $\xi_i\in[-0.5,+0.5]$, $\xi_i\in[-1,+1]$ were selected as an initial approximating basis from 50, 100 and 200 polynomial items. The structure of the approximating basis was selected in such a way that the argument exponents are close to 1. It is empirically known that this improves the extrapolation of the simulated values in the nodes (7).

Polynomials, rational functions and generalized polynomials are used for the approximation of functions as well [3]:

$$f(x)=\sum\nolimits_{j=1}^{L}a_j\varphi_j(x),$$

where: $f(x)$ – approximating function; $a_j$ – approximation coefficients; $\varphi_j(x)$ - functions with special properties, in particular, trigonometric and exponential functions; $n$ – number of functions. If $\varphi_j(x)$ is Legendre polynomial, then during its orthogonalization fractional-rational functions that are identical to polynomials with fractional exponents appear [4].

To find approximation coefficient $c_I^k$ using the data from expressions (8) and (9), we used identification problems regularized by minimizing the stabilizing Tikhonov functional [5] and reduction of the approximating basis [6, 7]. However, such approximation has an acceptable error of approximation only in the identification nodes (2), (4)

and beyond them deviates greatly from the approximated value in the points (7).

Thus, to restore the ionization field, additional measures were taken. An artificial argument that depends nonlinearly on x, y, z was added to the arguments of the polynomial:

$$P_k(x, y, z, r) = \sum_{|i+j+l+p| < R} c_{ijlp} x^{\lambda i} y^{\lambda j} z^{\lambda l} r^{\lambda p} \quad (10)$$

in particular:

$$r = \sqrt{(x_c^k - x)^2 + (y_c^k - y)^2 + (y_c^k - y)^2} \; ,$$

where $r$ – radius-vector; $x_c^k, y_c^k, z_c^k$ – center coordinates of the parallelepiped (7).

Identification problem intended to determine the polynomial coordinates for a separate calculation $k \in [1, K]$ has two conditions:

- approximation of values (9) in the points (8):

$$\min_{c_I^k} \sum_{a=1}^{A} \left[ v_a^k - P_k(x_a, y_a, z_a, r_a) \right]^2 + \alpha \sum_I \left( c_I^k \right)^2 \quad (11)$$

- minimization of the polynomial derivative $P_k$ with respect to its argument in the points (7)

$$\min_{c_I^k} \sum_{i,j,l,p=1}^{L} \left( 0 - \sum_{q=x,y,z,r} P_k^q(\hat{x}_i, \hat{y}_j, \hat{z}_l, \hat{r}_p) \right)^2 + \alpha \sum_I \left( c_I^k \right)^2 \quad (12)$$

where: $c_I^k$ – polynomial coefficients $P_k$; $I$ – their multi-indexes; $P_k^q$ – polynomial derivatives $P_k$ ( $q = x, y, z, r$ ):

$$P_k^x = \frac{\partial}{\partial x} P_k(x, y, z, r) \, ;$$

$$P_k^y = \frac{\partial}{\partial y} P_k(x, y, z, r) \, ;$$

$$P_k^z = \frac{\partial}{\partial x} P_k(x, y, z, r) \, ;$$

$$P_k^r = \frac{\partial}{\partial r} P_k(x, y, z, r) \cdot$$

To solve (11), (12), the reduction of the approximating basis described in [6-8] was used. To reduce the deviations of the approximating polynomial from the measured ionization values, the first-degree

(R = 1) polynomial was chosen and minor deviations $\lambda \in [0.7, 1.3]$ were applied [9-11].

Multiple solving of the problems (11) and (12) for all measured data $k = \overline{1, K}$ lead to such interim conclusions:

- if polynomial exponents of numerous arguments are close to 1, then approximation basis found using the reduction of the polynomial exponent while solving the problem (11), (12) for the values of an individual measurement $k$ (1)

$k \in [1, K]$ provides an acceptable approximation for all measurements $k = \overline{1, K}$ .

- if the exponent of the approximation polynomial differs greatly from 1 ($\lambda R > 1.5$, or $\lambda R < 0.5$), the reduction of the approximation polynomial exponent for each measurement leads to obtaining different approximation bases. This does not lead to substantial improvement of the approximation accuracy (10) and mostly makes the accuracy of the expression (12) worse.

From the results of these computational experiments, it can be concluded that to restore the ionization field, it is advisable to use the polynomial (10) with the exponent $R = 1$ and multiplier $\lambda$ that is slightly less than 1. For other conditions, we need substantial costs for computational resources to determine the approximation basis and coefficient $c_I^k$ for each of the measurements ( $k = \overline{1, K}$ ) separately.

## 5. Results of the Experimental Restoration of the Changes in the Atmosphere Ionization

To experimentally determine the changes in the ionization field in time, we took $k = 46$ measurements from 272 days in 2013, namely STEC values with time interval of 15 sec. during the first 12 minutes from the beginning of the day that were determined during the GNSS observations at 17 continuously operating stations of the ZAKPOS network [12].

For the most measurements ( $k = \overline{1, K}$ ), in case of the reduction of the approximation polynomial exponent, the same approximation basis was found.

The exponents of the polynomial arguments are given in the Table 1. The full set of coefficients of this approximation basis is determined using the parameters R = 1; $\lambda = 1.3^{-1}$; $|i+j+l+p| \leq 1$. Values of the approximation coefficients $c_I^1$ determined for a measurement at the time $t_1 = 0$ (the time is defined in the seconds of the day) are provided in the table as well.

The obtained solutions to the problems (11) and (12) are the coefficient values $c_i(t_k)$ ($i = \overline{1,n}$; $k = \overline{1,K}$) at the time $t_k$ where n = 6 – number of these coefficients.

Using cubic Hermite spline for interpolation (function pchip in Matlab), we obtained the approximation coefficients values for each second. Using the interpolation by the fifth-degree spline, their continuous values $c_i(t)$ (t∈[$t_1,t_k$] were determined. Fig. 4 shows the common dependencies of these approximation parameters from time.

Fig. 4a-c shows that parameters gradually change over time. This change depends on angle altitude of certain satellites and their ascent and descent, namely changes in number of satellites. Only one parameter $c_5(t)$ changes relatively very quickly (Fig. 4d). This indicates that the problem of restoration of $c_i(t)$ during t∈[$t_1,t_k$] using data (1) to determine the reduced (regularized) approximation basis common to all observations $k = \overline{1, K}$ is incorrect. However, the above solution shows that the change speed of $c_5(t)$ is limited. This fact confirms a good choice in the approximation basis for all observations $k = \overline{1, K}$ (during all time t∈[$t_1,t_k$]).

**Table 1    Exponents of the polynomial arguments determined for the most measurements and the values of the approximation coefficients $c_I^1$ for a measurement k = 1.**

| № | Exponent x | Exponent y | Exponent z | Exponent r | Coefficient $c_I^1$ |
|---|---|---|---|---|---|
| 1 | 0 | 0 | 0 | 0 | 7.623044 |
| 2 | 0 | 0 | 0 | 0.769231 | 0.004773 |
| 3 | 0 | 0 | 0.769231 | 0 | –0.000469 |
| 4 | 0 | 0.769231 | 0 | 0 | –0.003179 |
| 5 | 0.769231 | 0 | 0 | 0 | –0.010377 |
| 6 | 0 | 0 | –0.769231 | 0 | –6.092696 |



(a)



(b)



(c)



(d)
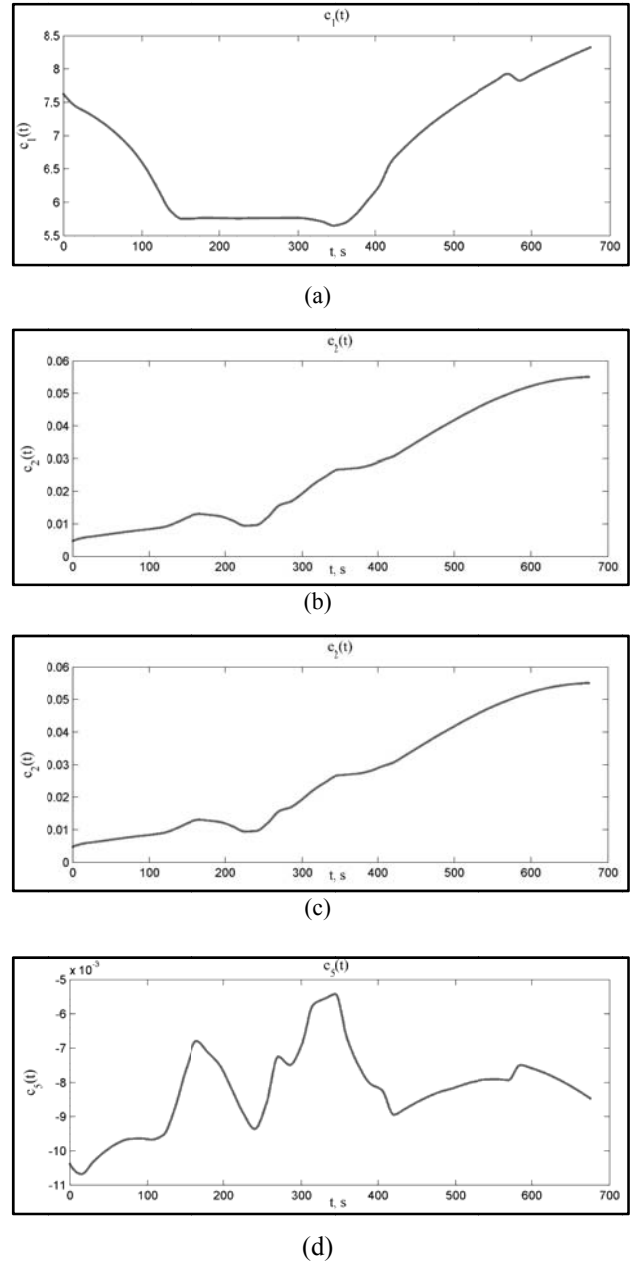
**Fig. 4    Time dependencies graph of approximation coefficients $c_1(t)$ (a), $c_2(t)$ (b), $c_3(t)$ (c), $c_5(t)$ (d).**

The quality analysis of the graphs $c_i(t)$ (t∈[$t_1,t_k$]) described above is applied to control the adequacy of the solution to the problem (11), (12) for all $k = \overline{1,K}$. In addition, to evaluate this solution, we applied quality analysis of the determined ionization distribution in the points (7). Acceptable solutions to (11) and (12) are distribution (probability density) of the needed ionization in the points (7) that has a central maximum

or is close to even or linear distribution. Fig. 5 shows common distribution graphs and functions of the ionization distribution $v(x, y, z, t_{12})$ determined using the polynomial (10) in the points (7).

It can be seen that all the restored ionization values are approximately equal to experimentally measured ionization values. Fig. 5 also illustrates a common result of using the approximation basis (see Table 1) determined in one point ($k = 2$) to restore ionization in another point ($k = 12$). Such quality analysis of distribution laws for ionization approximation in the points (7) is applied to all measurements $k = \overline{1, K}$.

To restore the change in the ionization field, we need to determine continuous dependencies of the area center coordinates (7) $x_c(t)$, $y_c(t)$, $z_c(t)$ ($t \in [t_1, t_k]$) from time using approximation by spline. Graphs of the coordinate changes are shown on Fig. 6.

Fig. 6 shows the shifts of the center of the rectangular area with irregular fluctuations. This can be explained by the movement of satellites and discrete division of sub-ionospheric line segment of the beam from the station to satellite. This indicates that the ionization field depends on the algorithm parameters.
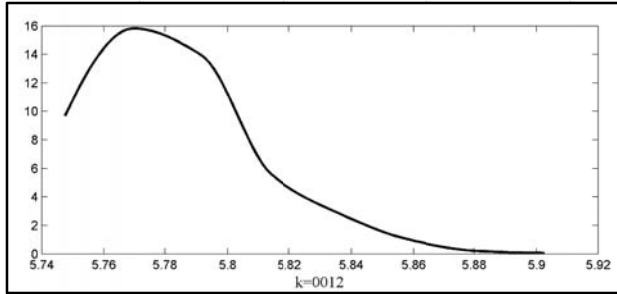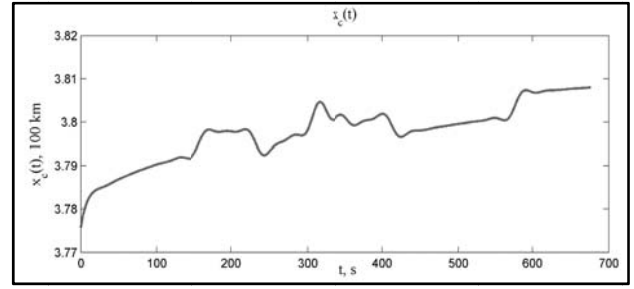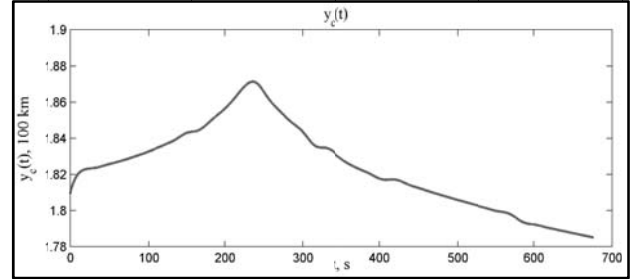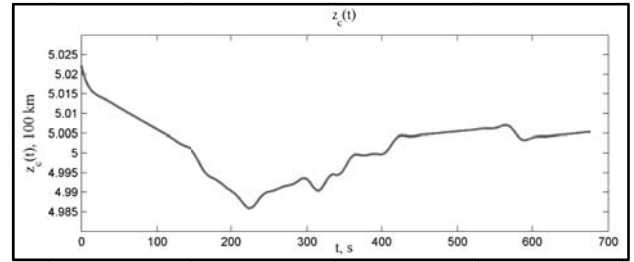


(a)
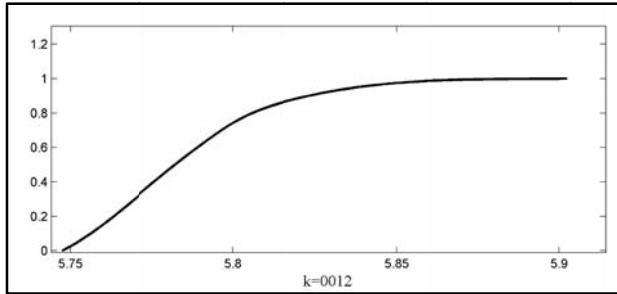


(b)

**Fig. 5 Common view of graphs for probability density (a) and distribution function (b) of the ionization value $v(x, y, z, t_{12})$ restored in the rectangular area (14).**



(a)



(b)



(c)

**Fig. 6 Time dependency graphs of the center of the ionization restoration area $x_c(t)$ (a), $y_c(t)$ (b), $z_c(t)$ (c).**

It should be noted that the area boundaries (7) change gradually depending on the satellite movements. Common graphs of change $x_{\min}(t_k) = x_{\min}^k$; $y_{\min}(t_k) = y_{\min}^k$; $z_{\min}(t_k) = z_{\min}^k$; $x_{\max}(t_k) = x_{\max}^k$; $y_{\max}(t_k) = y_{\max}^k$; $z_{\max}(t_k) = z_{\max}^k$ ($k = \overline{1, K}$) are shown on Fig. 7.

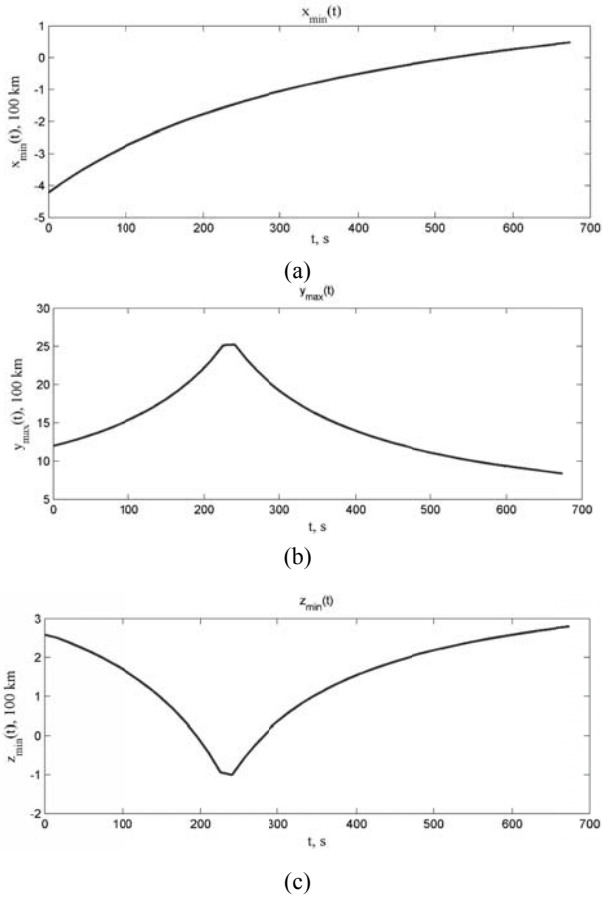Extreme values of these boundaries were defined for the ionization field restoration:

$$\overline{x}_{\min} = \max_{k \in [1, K]} x_{\min}^k; \quad \overline{y}_{\min} = \max_{k \in [1, K]} y_{\min}^k; \quad \overline{z}_{\min} = \max_{k \in [1, K]} z_{\min}^k;$$

$$\overline{x}_{\max} = \min_{k \in [1, K]} x_{\max}^k; \quad \overline{y}_{\max} = \min_{k \in [1, R]} y_{\max}^k; \quad z_{\max} = \min_{k \in [1, K]} z_{\max}^k.$$

They describe rectangular area

$$x \in [\overline{x}_{\min}, \overline{x}_{\max}], \quad y \in [\overline{y}_{\min}, \overline{y}_{\max}], \quad z \in [\overline{z}_{\min}, \overline{z}_{\max}] \quad (13)$$

for which the ionization values during the whole period of observations $t \in [t_1, t_k]$ are restored.

(a)

(b)

(c)

**Fig. 7    Common view of time dependency graphs of the changes in boundaries of the ionization restoration area: $x_{min}(t)$ (a), $y_{max}(t)$ (b), $z_{min}(t)$ (c).**

Let's divide the line segments (13) into $L\text{-}1$ segments and determine the coordinate values for equally located nodes:

$$\hat{x}_i, \hat{y}_j, \hat{z}_l \ (i,j,l = \overline{1,L}). \quad (14)$$

Ionization values in the nodes (14) are computed using the polynomial (10) with parameters $c_i(t)$ ($i = \overline{1,n}$), $x_c(t)$, $y_c(t)$, $z_c(t)$, that depend on time:

$$v(x,y,z,r) = \sum_{ijlp} c_{ijlp}(t) x^{\lambda i} y^{\lambda j} z^{\lambda l} r^{\lambda p} \quad (15)$$

where: $i, j, l, p$ are the indexes of the polynomial coefficients. The exponents of its arguments are determined beforehand based on computational experiments conducted when solving the problems (11) and (12) (see Table 1). The common view of graph that shows the instantaneous value of the ionization field restored in the nodes (14) is illustrated on Fig. 8. In

formula (15), continuous time functions $c_i(t)$ ($i = \overline{1,n}$), $x_c(t)$, $y_c(t)$, $z_c(t)$, are defined using splines. According to formula (15), we determine the ionization at an arbitrary time $t \in [t_1, t_k]$ in the arbitrary point (13). It was found that most often, the ionization increases with an altitude and there is a shift of spherical areas with reduced or increased ionization. Sometimes such areas stop shifting and start moving in the opposite direction and mix. Restoring the spatial dynamics of ionization (15) models complex processes of electric charge movements in the ionized air.

The described method is based on the interpolation of the coefficients of the polynomial from numerous arguments (10). It can be used for data in (8) and (9) that leads to the same reduced approximation basis. This method is described briefly in the algorithm at the end of the article (see chapter 5).

Using this algorithm, the results of the ionization field restoration were obtained. In particular, this algorithm was applied with the following parameters: number of points on the beam from the station to satellites $N = 3$; number of points between the points on different beams $M = 1$. With such parameters in the expression (11), the number of approximation nodes exceeds 55 thousand. Number of nodes along the area boundary of the ionization restoration is $L = 20$. Using this value, the number of minimization nodes of the
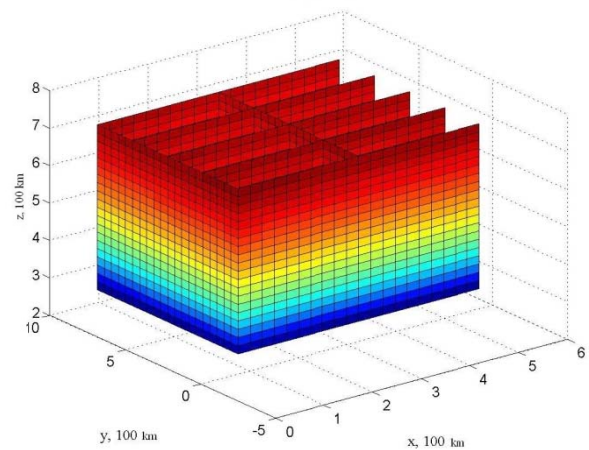


**Fig. 8    Graphs of the ionization dependency from the spatial coordinates (in 100 km) in the moment ($t_{38} = 555$ s).**

derivative by the polynomial from numerous arguments in (12) is 9261. An increase in the above-mentioned parameters causes severe computation complications in problems (11) and (12) and does not improve the accuracy of its solution.

Statistical characteristics, that describe 46 results of the solution to the problem (11) and (12), ( $k = \overline{1, K}$ , $K = 46$), are provided in Table 2.

This table shows such characteristics:

- standard deviation (SD) of the absolute approximation error in 46 results of the problem (11);
- SD of the relative approximation error in 46 results of the problem (11);
- average ionization in the approximation nodes (8) computed for 46 moments in observation from polynomial (10);

- average ionization in the approximation nodes (experimental values from 46 observational moments) (9);
- average relative approximation error by module for 46 solutions to the problem (11).

For these characteristics, such parameters were computed: the smallest, largest and average value, median, distribution mode, standard deviation of the accuracy identifier as a set of its 46 values. The first two rows of the last column show the standard deviation of the SD of 46 approximation problems (11). These parameters describe the accuracy of application of common approximation basis (see Table 1) in order to restore the changes in the ionization field in time.

**Table 2   Statistical characteristics for 46 results of the solution to the problem (11) obtained using common approximation basis.**

| Name of identifier | Parameters | | | | | |
|---|---|---|---|---|---|---|
| | The smallest value | The biggest value | Average value | Median | Distribution mode | SD |
| SD of the absolute approximation error in (11) | 1.3892 | 1.4652 | 1.4198 | 1.4226 | 1.3892 | 0.016779 |
| SD of the relative approximation error in (11) | 0.15017 | 0.15737 | 0.15247 | 0.15230 | 0.15017 | 0.001354 |
| Average ionization in the approximation nodes (8) computed from polynomial (10) | 5.7050 | 5.8206 | 5.7377 | 5.7354 | 5.7050 | 0.021957 |
| Average ionization in the approximation nodes (8), experimental values (9) | 5.7049 | 5.8206 | 5.7377 | 5.7352 | 5.7049 | 0.021971 |
| Average relative approximation error (11) (by module) | 0.21556 | 0.22512 | 0.21967 | 0.22016 | 0.21556 | 0.002148 |

In particular, Table 2 shows that the average values of the experimental and model (obtained from approximation) values are close for all measurements. The relative accuracy of the problem (11) solution for an individual measurement is approximately 21% (with dispersion 0.21% for all measurements). The standard deviation of this error is 15% (with dispersion 0.13% for all measurements). This means that using the common approximation basis, we obtained ionization approximation (11) with relatively low accuracy (21%) but the error of such approximation varies a little for

each of the measurements. This proves the efficiency of applying the common approximation basis for regularized approximation of the atmosphere ionization when using the polynomial from numerous arguments with coefficients dependent on time. It should be noted that before we added a new argument to the polynomial (10), the approximation accuracy was worse. Other ways to expand or change the approximation basis (described above) do not influence the accuracy parameters for ionization field restoration.

## 6. Algorithm of the Ionization Field Change Restoration Using the Approximation of the Change in Time of the Coefficients of the Polynomial from Numerous Arguments

(1) Obtain the coordinates of the stations (1a), satellites (1b) and STEC values (1c).

(2) Determine the altitude of the sub-ionospheric point.

(3) Select a number of points $N$ on the beams from the stations to satellites located lower than the sub-ionospheric point.

(4) Compute (2) the coordinates $\overline{x}_{ijl}^k$, $\overline{y}_{ijl}^k$, $\overline{z}_{ijl}^k$ of the points located on the beams between the stations and satellites lower the sub-ionospheric point ($i = \overline{1, n_k}$; $j = \overline{1, m_k}$; $l = \overline{1, N}$; $k = \overline{1, K}$).

(5) Compute (3) the value $\overline{v}_{ijl}^k$ in the points (2) (located on the beams between the stations and satellites lower than the sub-ionospheric point) that are defined in step 4 ($i = \overline{1, n_k}$; $j = \overline{1, m_k}$; $l = \overline{1, N}$; $k = \overline{1, K}$).

(6) Select a number of internal nodes located on the line segments between two points on the beams from stations to satellites.

(7) Compute coordinates of internal nodes $\breve{x}_{ijpq}^{kr}$, $\breve{y}_{ijpq}^{kr}$, $\breve{z}_{ijpq}^{kr}$ (4) that lie on the segments between two points on the beams from stations to satellites ($r = \overline{1, M}$; $p, q \in [1, N]$; $i = \overline{1, n_k}$; $j = \overline{1, m_k}$; $k = \overline{1, K}$).

(8) Using interpolation determine $\breve{v}_{ijpq}^{kr}$ (5) in the points defined in steps 6 and 7 ($i = \overline{1, n_k}$; $j = \overline{1, m_k}$; $p, q \in [1, N]$; $r = \overline{1, M}$; $k = \overline{1, K}$).

(9) Determine boundaries $x_{\min}^k$, $y_{\min}^k$, $z_{\min}^k$, $x_{\max}^k$, $y_{\max}^k$, $z_{\max}^k$ (6) of the rectangular spatial area with the points $\overline{x}_{ijl}^k$, $\overline{y}_{ijl}^k$, $\overline{z}_{ijl}^k$ (2) and defined values $\overline{v}_{ijl}^k$ (3) ($i = \overline{1, n_k}$; $j = \overline{1, m_k}$; $l = \overline{1, N}$) for each measurement ($k = \overline{1, K}$).

(10) Select a number of points $L$ where the spatial area is divided and limited by the boundaries (6) set in step 9.

(11) In the rectangular area defined in step 9 determine the coordinates of the equally located points $\widehat{x}_i^k$, $\widehat{y}_j^k$, $\widehat{z}_l^k$ (7) ($i, j, l = \overline{1, L}$).

(12) Join the sets of the nodes coordinates on the beams from stations to satellites (2) and on these beams (4) and sets of the correspondent known values (3), (5) into a combined set $x_a^k$, $y_a^k$, $z_a^k$, $v_a^k$ (8), (9) ($a = \overline{1, A_k}$) that is experimentally defined discrete functional dependency of the ionization from spatial coordinates for a measurement k ($k = \overline{1, K}$).

(13) Determine the best approximation basis common for all measurements $k = \overline{1, K}$ from the results of the problems (11), (12), exponent reduction of the polynomial from numerous arguments (10) [3, 4].

(14) Solve the problem (11), (12) for all measurements $k = \overline{1, K}$ using approximation basis determined in step 13.

(15) Based on the results from step 14, using the interpolation by spline, define coefficient dependencies $c_i(t)$ ($i = \overline{1, n}$) of the polynomial (10) from time and dependency of the center coordinates $x_c(t)$, $y_c(t)$, $z_c(t)$ of the rectangular area (7) from time ($t \in [t_1, t_k]$).

(16) Make a quality analysis of changes in the polynomial (10) coefficient $c_i(t)$ ($i = \overline{1, n}$) in time ($t \in [t_1, t_k]$).

(17) Define approximation errors in the problem (11) for all measurements.

(18) Make a quality analysis of the probability density (and distribution function) of the restored ionization value $v(x, y, z, t)$ in points (7) in the rectangular area (6). If these distributions have central maximum or are approximately even or linear, and if approximation errors in the problem (11) for all measurements are within acceptable limits then the determined approximation basis (step 13) can be regarded as acceptable. Otherwise, go to step 3.

(19) Define the boundaries $\left[\overline{x}_{\min}, \overline{x}_{\max}\right]$, $\left[\overline{y}_{\min}, \overline{y}_{\max}\right]$, $\left[\overline{z}_{\min}, \overline{z}_{\max}\right]$ (13) of the rectangular area (14) where the approximation value of the ionization for all measurements $k = \overline{1, K}$ is computed.

(20) Determine the coordinates of the equally located points $\hat{x}_i, \hat{y}_j, \hat{z}_l$ in the rectangular area defined in step 18 ($i, j, l = \overline{1, L}$).

(21) Using the coefficients $c_i(t)$ ($i = \overline{1, n}$) in the polynomial (10) and the center coordinates $x_c(t)$, $y_c(t)$, $z_c(t)$ of the rectangular area (13) that depend on time, determine the ionization value $v(x, y, z, t)$ at an arbitrary time $t \in [t_l, t_k]$ in the arbitrary point of the area (13).

(22) To represent the results of the ionization restoration graphically, compute the ionization values in the points (14), i.e., compute $v(\hat{x}_i, \hat{y}_j, \hat{z}_l, t)$ ($i, j, l = \overline{1, L}$; $t \in [t_l, t_k]$).

## 7. Conclusion

The resulting error indicators show that the developed algorithm gives consistent results for ionization field restoration that do not depend on the ionosphere state, satellites positions and changes in number of stations in the network used for computations. Instant accuracy of the ionization field restoration is acceptable for our problem. To improve the described method, we need to conduct research to explain the structure of the approximating polynomial and search for additional computation tools to increase the approximation accuracy in the observational nodes and prevent rapid change of the approximating polynomial beyond these nodes.

## References

[1] Kalman, R. E., Falb, P. L., and Arbib, M. A. 1969. Topics in Mathematical System Theory. McGraw-Hill, New York.

[2] Zadeh, L., and Dezoer, I. 1963. Linear System Theory: The State Space Approach, McGraw-Hill, NY.

[3] Vladimirov, V. S. 1981. Equations of Mathematical Physics. V. S. Vladimirov, Moscow: Nauka, p. 512.

[4] Vasyliev, V. V., and Symak, L. A. 2008. "Fractional Calculus and Approximation Methods in the Modeling of Dynamic Systems". Scientific Publication, V. V. Vasyliev, L. A. Symak, Kyiv, The National Academy of Sciences of Ukraine, p. 256.

[5] Tikhonov, A. N., and Arsenin, V. Y. 1979. Solutions of Ill-Posed Problems. Moscow: Nauka, p. 288.

[6] Matviichuk, Y. M. 2000. Mathematical Macro-Modeling of Dynamic Systems: Theory and Practice. Lviv: Publishing House of Ivan Franko National University of Lviv, p. 215.

[7] Matviichuk, Y. M., Kurhanevych, A., Olyva, O., Pauchok, V. 2000. "Prognostic Modeling of Dynamic Systems (Macro-Model Approach)". In: Automatics 2000: International Conference, Lviv, September 11-15, 2000, Vol. 7, pp. 82-87, 232.

[8] Yankiv-Vitkovska, L. M., Matviichuk, Y. M., Savchuk, S. H., and Pauchok, V. K. 2012. "The Research of Changes of GNNS Stations Coordinates by the Method of Macromodelin." Geodesy and Cartography Bulletin 1 (78): 9-17.

[9] Verlan, A. F., and Fedorchuk, V. A. 2013. Models of the Dynamics of Electromechanical Systems. The National Academy of Sciences of Ukraine, Pukhov Institute for Modeling in Energy Engineering. Kyiv: Naukova Dumka, p. 222.

[10] Malachivskyy, P. S. 2009. "Mathematical Modeling of Functional Relationships between Physical Quantities Using Continuous and Smooth Minimax Spline Approximations". The thesis is presented for Dr. Tech. Sci. of the 01.05.02 specialty "Mathematical modeling and computing methods". Lviv Polytechnic National University, Lviv.

[11] Malachkivskyi, P. S. 2013. Continuous and Smooth Minimax Spline Approximation. Ukraine, Glushkov Institute of Cybernetics; Mathematical Modeling Center of the Pidstryhach Institute for Applied Problems of Mechanics and Mathematics. Kyiv: Naukova Dumka, p. 271.

[12] Yankiv-Vitkovska, L. M. 2013. "Methods of Determining the Ionosphere Parameters in the Network of Satellite Stations in the Western Ukraine". Space Science and Technology 19 (6): 47-52.